Classification: Original article

THE TRANSMEMBRANE DOMAIN OF PODOPLANIN IS REQUIRED FOR ITS ASSOCIATION WITH LIPID RAFTS AND THE INDUCTION OF EPITHELIAL-MESENCHYMAL TRANSITION

Beatriz Fernández-Muñoz[a,1], María M. Yurrita[a], Ester Martín-Villar[a,2], Patricia Carrasco-Ramírez[a], Diego Megías[b], Jaime Renart[a,*], Miguel Quintanilla[a]

[a]Instituto de Investigaciones Biomédicas Alberto Sols, Consejo Superior de Investigaciones Científicas (CSIC)-Universidad Autónoma de Madrid (UAM), 28029-Madrid, Spain.

[b]Centro Nacional de Investigaciones Oncológicas, 28029-Madrid, Spain.

[*]Corresponding autor at: Instituto de Investigaciones Biomédicas Alberto Sols, CSIC-UAM, Arturo Duperier 4, 28029-Madrid, Spain. Tel.: +34 91 5854439; fax: +34 91 5854401

E-mail address: jrenart@iib.uam.es (J. Renart).

[1]Present address: Laboratorio Andaluz de Reprogramación Celular. Parque Tecnológico y Científico Cartuja 93. 41092-Sevilla, Spain

[2]Present address: Randall Division of Cell and Molecular Biophysics, King's College London, Guy's Campus, SE1UL, UK.

ABSTRACT

Podoplanin is a transmembrane glycoprotein that is upregulated in cancer and was reported to induce an epithelial-mesenchymal transition (EMT) in MDCK cells. The promotion of EMT was dependent on podoplanin binding to ERM (ezrin, radixin, moesin) proteins through its cytoplasmic (CT) domain, which led to RhoA-associated kinase (ROCK)-dependent ERM phosphorylation. Using detergent-resistant membrane (DRM) assays, as well as transmembrane (TM) interactions and ganglioside GM1 binding, we present evidence supporting the localization of podoplanin in raft platforms important for cell signalling. Podoplanin mutant constructs harbouring a heterologous TM region or lacking the CT tail were unable to associate with DRMs, stimulate ERM phosphorylation and promote EMT or cell migration. Similar effects were observed upon disruption of a GXXXG motif within the TM domain, which is involved in podoplanin self-assembly. In contrast, deletion of the extracellular (EC) domain did not affect podoplanin DRM association. Together, these data suggest that both the CT and TM domains are required for podoplanin localization in raft platforms, and that this association appears to be necessary for podoplanin-mediated EMT and cell migration.

Key words: Podoplanin, DRMs, Lipid rafts, Transmembrane domain, GXXXG motif, EMT

Abbreviations: Cav-1, Caveolin-1; CD, Methyl-β-Cyclodextrin; CT, Cytoplasmic; CTB, Cholera Toxin B-subunit; DRM, detergent-resistant membrane; EC, Extracellular; E-CD, E-Cadherin; EMT, ENAC, Epithelial Sodium Channel α subunit; Epithelial-to-Mesenchymal Transition; ERM, Ezrin, Radixin, Moesin; PDPN, Podoplanin; ROCK, RhoA-associated kinase; TM, Transmembrane.

1. Introduction

Podoplanin (PDPN), also called PA2.26 antigen, Aggrus, and T1α, is a small membrane mucin-like type I glycoprotein expressed in mesothelia, osteoblasts, osteocytes, certain types of neurons, and several epithelia (Wicki and Christofori, 2007). It is also expressed in the lymphatic but not blood vessel endothelium, making podoplanin a useful immunohistochemical marker for lymphangiogenesis analysis (Ordonez, 2006). Studies with podoplanin-deficient mice have revealed it plays an important role for this glycoprotein in the morphogenesis of the lung (Ramirez et al., 2003), the formation of the lymphatic vasculature (Schacht et al., 2003) and cardiac development (Mahtab et al., 2008). Nevertheless, the precise biological function of podoplanin in normal tissues remains to be elucidated.

Podoplanin is upregulated in a variety of cancers, and has been recently identified as a candidate cancer stem cell marker in squamous cell carcinomas (Atsumi et al., 2008). The general consensus about the role of podoplanin in cancer is that it promotes tumor cell migration, invasion and metastasis (Wicki and Christofori, 2007).

The human podoplanin precursor polypeptide is 162 amino acids long. It is composed of an O-glycosylated EC domain followed by a hydrophobic TM segment and a CT tail of only nine amino acids (Martin-Villar et al., 2005). The EC region contains three repeats (PLAG domains) that have been shown to induce tumor-platelet aggregate formation and facilitate pulmonary metastasis (Kunita et al., 2007). We have shown that in premalignant keratinocytes and MDCK cells podoplanin induces an EMT that is associated with increased migration/invasion and lymph node metastasis (Scholl et al., 1999; Scholl et al., 2000; Martin-Villar et al., 2005; Martín-Villar et al., 2006). Podoplanin binds ezrin/moesin members of the ERM protein family through basic residues of its CT domain linking it to the actin cytoskeleton. This interaction is crucial for podoplanin-mediated activation of the small

GTPase RhoA and its associated kinase ROCK, thereby promoting an EMT (Martín-Villar et al., 2006). On the other hand, Wicki and coworkers (2006) reported that podoplanin is able to stimulate collective tumor cell migration/invasion in the absence of EMT by inducing a rearrangement of the actin cytoskeleton. These studies point to a crucial role of the EC and CT domains in podoplanin-induced cell adhesion and motility, respectively.

Recently, Barth and colleagues (2010) have shown that podoplanin/T1α is associated with lipid raft micro domains in microvillar protrusions of lung alveolar epithelial cells. Raft constituents are normally present in the detergent-resistant membrane (DRM) fraction after non-ionic detergent solubilization at 4ºC. They are dynamic nanoscale assemblies of sphingolipids, cholesterol and proteins that can be stabilized into larger platforms and are involved in viral infection, membrane trafficking and signal transduction (Simons and Gerl, 2010). In the present work, we have analyzed the involvement of the TM domain of podoplanin on its localization in DRMs and in the promotion of EMT.

2. Materials and methods

2.1. Constructs

Constructs for enhanced green fluorescent protein (eGFP) fusion proteins of wild-type podoplanin (PDPN-WT), PDPN-ΔCT and PDPN-ΔEC have been described elsewhere (Martín-Villar et al., 2006). Constructs for TM chimeric and GXXXG mutants are described in detail in the Supplementary material section, including the oligonucleotides used for their amplification (Table S1). All PCR-derived constructs were confirmed by sequencing.

2.2. Cell culture conditions and cDNA transfections

We used in this study MDCK type II cells, which do not express podoplanin (Zimmer et al., 1997; Zimmer et al., 1999; Martín-Villar et al., 2006). Cell culture conditions and plasmid transfections were as previously described (Martin-Villar et al., 2005). MDCK cell transfectants were selected with 0.5 mg/ml G418 (Promega Biotech Ibérica) for 2 weeks, and individual clones expressing podoplanin selected by sorting and flow cytometry. All experiments were performed with at least two different clones for each construct, yielding similar results.

2.3. Detergent insolubility and OptiPrep™ density gradient assays

Triton X-100 insolubility assays were performed as described (Neame and Isacke, 1992), with slight modifications. Briefly, confluent cell monolayers were washed twice in cold Tris-saline buffer (15 mM Tris-HCl, pH 7.5, 120 mM NaCl), scraped in 400 μl of cold extraction buffer (5 mM Tris-HCl, pH 7.5, 1 mM $CaCl_2$, 1 mM $MgCl_2$, 150 mM NaCl, 0.2% Triton X-100, plus protease inhibitors), and incubated on ice for 10 min. Lysates were centrifuged at 18 000×*g* at 4ºC for 15 min to separate Triton-insoluble material. The supernatant was designed as the soluble fraction.

For flotation experiments in OptiPrep™ density gradients, cells were washed in cold PBS, lysed in TNE buffer (50 mM Tris-HCl, pH 7.4, 150 mM NaCl, 5 mM EDTA, 0.5% Triton X-100, plus protease inhibitors) and incubated on ice for 20 min, as described by Gomez-Mouton et al. (2001). Cells were then scraped and passed several times through a 25-gauge needle. Samples were brought to 35% (v/v) with cold OptiPrep™ (Sigma-Aldrich) in TNE buffer (0.5 ml final volume), transferred into SW60 centrifuge tubes, overlaid with 3.5 ml of 30% OptiPrep™ in TNE buffer and 200 μl of TNE buffer, and centrifuged for 4 h at

170 000×*g* at 4ºC. Eight 0.5 ml fractions were collected from the top of the gradient. The presence of podoplanin and raft markers in the fractions was analyzed by Western blotting. Density gradients for mutant podoplanin proteins were run in parallel to wild type podoplanin as a control.

For cholesterol depletion, cells were washed in PBS and incubated with 20 mM methyl-β-cyclodextrin (CD, Sigma-Aldrich) in serum-free medium at 37ºC for 30 min. After incubation, CD was washed with serum-free medium containing 0.01 % BSA. In these conditions, ~90% of cholesterol is removed from MDCK cells (Francis et al., 1999).

2.4. Western blot analysis

Total cell lysates and Western blot analysis were performed as previously described (Martín-Villar et al., 2006). To detect podoplanin, an antibody raised against the peptide 37-51 (P37-51) of the EC domain was used, and its specificity was verified by preincubating with an excess of this peptide (Martin-Villar et al., 2005). For podoplanin detection in OptiPrep™ density gradients, the commercial mAb NZ-1 (Acris antibodies) was used. Expression of CD44 was analyzed under non-reducing conditions with the rat mAb IM7, kindly provided by Helen Yarwood (The Institute for Cancer research, London, UK). Antibodies for phospho-ERM and caveolin-1 (Cav-1) were from Cell Signaling Technology and BD Biosciences, respectively. Antibodies for ezrin (3C12), eGFP and α-tubulin (DM1A) were from Sigma-Aldrich, and mAbs for N-cadherin and CK8 were from Zymed Laboratories. The mAb ECCD-2 was used for E-cadherin detection. Appropriate horseradish-peroxidase-conjugated secondary antibodies were used.

2.5. Bead assay

Five μm in diameter polystyrene beads (Duke Scientific Corporation) were coated with 10 μg/ml of cholera toxin B-subunit (CT-B) conjugated with Alexa Fluor-594 (Calbiochem) or a polyclonal antibody (sc-9099, Santa Cruz Biotechnology) directed against the EC domain of the transferrin receptor, as described by del Pozo et al. (2004). Cells seeded on coverslips were washed with serum-free culture medium and incubated with coated beads (cell to bead ratio of 1:10) at 37ºC for 15 min. Cells were then washed three times with PBS to remove excess beads, and fixed/processed for immunofluorescence analysis.

2.6. Fluorescence and confocal microscopy analysis

Immunofluorescence detection of proteins was performed in cells fixed with 3.7% formaldehyde in PBS and permeabilized with 0.05% Triton X-100. For E-cadherin and CD44 staining, the mAbs ECCD-2 and HP2/9 (a generous gift of F. Sánchez-Madrid, Hospital Universitario La Princesa, UAM), respectively, were used. Secondary antibodies were Alexa Fluor 594-labeled anti-rabbit or anti-mouse IgGs (Molecular Probes). Phalloidin coupled to Alexa Fluor 594 was used for F-actin staining. Nuclei were stained with a 1 μg/ml solution of 4',6-diamino-2-phenilindole (DAPI; Sigma-Aldrich). In vivo podoplanin pre-embedding staining was performed as previously described (Martín-Villar et al., 2006). Confocal laser-scanning microscopy was performed in a TCS-SP2 microscope (Leica Microsystems). Images were taken using a 63x (NA1.32) oil-immersion objective and assembled using the Leica Confocal Software 2.0 or Adobe® Photoshop® CS2.

2.7. Cell migration assays and time-lapse microscopy

Wound healing assays were performed as described previously (Scholl et al., 1999). Images of the wounds were taken at 0 and 12 h after wounding, and quantification of migrated cells was done by measuring the number of pixels in the wounded area using Adobe® Photoshop®. For Transwell assays, cells were seeded ($5x10^3$ cells/well) in DMEM containing 0.1% FBS and allowed to transmigrate for 6 h at 37ºC using 5% FBS as a chemoattractant. Cells on the upper side of the Transwell were then removed and those on the underside were fixed and stained with DAPI. Cell migration was quantified by counting the number of cells that migrated through the inserts. Four different fields per well were counted using an Axiophot fluorescence microscope (Carl Zeiss).

Random migration analysis was performed with time-lapse fluorescence microscopy. Cells grown at low confluence were maintained at 37ºC in a 5% CO_2 atmosphere. Images were taken every 5 min for 15 h with a Leica DMI6000B inverted fluorescence microscope (Leyca Microsystems) using a 10x objective. Cells entering or exiting the field, and those that divided during the time-lapse recording were excluded from the analysis. Images were processed, assembled into movies, and analyzed with Imaris 6.4.2 software. The following migration parameters were calculated: mean speed = total path length / time; displacement = distance between the starting and ending points of cell path; directionality = displacement / total path length.

2.8. TOXLUC assay

PDPN constructs, as well as the M1 TM segment of the human epithelial sodium channel α subunit (ENAC) from pKB52 (Kashlan et al., 2006), cloned in the TOXCAT vector pML27 (Lis and Blumenthal, 2006) were engineered to substitute the CAT gene for the luciferase gene (see supplementary material). Both plasmids were kindly provided by K.

Blumenthal (State University of New York, Buffalo, NY 14214, USA). Stationary phase cultures of the different E. coli strains were diluted 100-fold in prewarmed LB broth containing 50 μg/ml spectinomycin. After incubating at 37ºC for 3 h in a shaker water bath at 250 rpm, aliquots of 100 μl (per triplicate) were taken from the cultures and centrifuged at 14 000 rpm for 1 min. Pellets were resuspended in 100 μl of 100 mM potassium phosphate, pH 7.8, 2 mM EDTA, and cells lysed by freezing and thawing. Luciferase activity was determined using 5 μl of the cell extract and 20 μl of substrate (Promega Biotech Ibérica). Results are expressed as RLU per μg of protein.

2.9. Statistics

Data are presented as mean ± s.e.m. Significance was determined using one-way analysis of variance (ANOVA) with a Bonferroni post-test or the Student's *t*-test. All statistical analyses were performed using GraphPad Prism 4.0 software.

3. Results

3.1. Human podoplanin expressed in MDCK cells is associated with the detergent-insoluble membrane fraction

When the insolubility of human podoplanin (expressed in MDCK cells as a fusion protein with eGFP) in cold non-ionic detergent was tested, we found that a substantial amount of podoplanin was insoluble at detergent concentrations of 0.2-0.5 % (Fig. 1A, B). Podoplanin was detected together with CD44 and Cav-1, two well established raft markers (Patra, 2008), in the low density DRM fraction isolated by flotation in OptiPrep^{TM} density gradients.

Treatment of the cells with methyl-β-cyclodextrin (CD) to sequester cholesterol before fractionation rendered most podoplanin, CD44 and Cav-1 soluble (at the bottom of the gradients), confirming the presence of these proteins in cholesterol-enriched DRMs (Fig. 1B). Furthermore, cell surface cholesterol depletion by CD treatment caused a redistribution of podoplanin and CD44 from microvilli to the entire cell surface (Fig. S1 in Supplementary material) as expected from the fact that cholesterol extraction from the plasma membrane reduces the number and length of microvilli (Poole et al., 2004). We found that podoplanin colocalizes at microvilli with the ganglioside GM1, but not with Cav-1 (data not shown), confirming the results of Barth and colleagues (2010). Since cholera toxin B-subunit (CTB)-coated beads promote clustering of GM1-containing lipid rafts (del Pozo et al., 2004), we analyzed the effect of CTB-coated beads on podoplanin distribution at the cell surface. CTB-mediated membrane clustering of GM1 led to the recruitment of both podoplanin and CD44. In contrast, beads coated with an antibody recognizing the transferrin receptor (αTrfR), a non-raft protein, were shown to have no effect on the distribution of PDPN (Fig. 1C).

3.2. The TM domain of podoplanin is required for DRM association

It has been shown that association with DRMs is an intrinsic characteristic of some proteins that is often determined by their TM domain (Scheiffele et al., 1997). Therefore, we examined the effect of replacing the TM domain of podoplanin with that of the adherens junction protein E-cadherin (ECD), the leukocyte common antigen CD45, or the Toll-like receptor TLR9 on its association with DRMs. Whereas ECD and CD45 are cell-surface proteins, TLR9 localizes at the endoplasmic reticulum and endosomes (Leifer et al., 2004). Wild-type podoplanin (PDPN-WT) and the chimeric constructs fused to eGFP (PDPN-ECD, PDPN-CD45, PDPN-TLR9) were stably expressed in MDCK cells and their sub cellular

localization was analyzed by confocal microscopy (Fig. 2). In order to distinguish the proteins confined at the cell surface, the overall eGFP fluorescence signal was compared with the signal obtained after in vivo pre-embedding staining using a specific antibody recognizing the EC domain of podoplanin. PDPN-WT and PDPN-ECD were mainly directed to the cell surface, where they concentrated at membrane protrusions. Although some PDPN-CD45 had a perinuclear localization (likely at the Golgi apparatus), a substantial amount of this chimera also reached the plasma membrane but was distributed more homogeneously than PDPN-WT and PDPN-ECD. In contrast, most of PDPN-TLR9 was retained in the cytoplasm, accumulating at intracellular vesicles (Fig. 2, inset). We confirmed the cytoplasmic localization of PDPN-TLR9 by flow cytometry analysis (Fig. S2 in Supplementary material).

Substitution of the TM domain of podoplanin led to decreased detergent insolubility (Fig. 3A) and exclusion from the DRM fractions isolated by OptiPrep^{TM} density gradients (Fig. 3B). Moreover, these mutants were not recruited by CTB-coated beads (Fig. S3 in Supplementary material). A similar effect was found for a podoplanin mutant that lacked the CT tail (PDPN-ΔCT), while deletion of the EC domain (PDPN-ΔEC) did not affect podoplanin association with the DRM fraction (Fig. 3A, B). These results suggest that both the TM and CT domains of podoplanin are important for its localization in lipid rafts. We also analyzed the detergent insolubility properties of a podoplanin isoform lacking two amino acids (YS) of the CT tail (PDPN-ΔYS), which originates by alternative splicing and is normally expressed in human tissues (Martin-Villar et al., 2009). Most of PDPN-ΔYS was found in the insoluble fraction (Fig. 3A) and its flotation on OptiPrep^{TM} density gradients was only slightly affected (Fig. 3B).

3.3. The TM domain is required for podoplanin-mediated epithelial cell plasticity and migration

PDPN-WT expression in MDCK cells induced ROCK-dependent phosphorylation of ERM proteins and led to EMT associated with upregulation of N-cadherin and downregulation of E-cadherin expression. The capacity of PDPN-WT to induce an EMT in MDCK cells depends on the CT, but not the EC domain. Indeed, (Martín-Villar et al., 2006). Interestingly, podoplanin TM chimeric mutants, when expressed in MDCK cells at similar or higher levels than PDPN-WT, were unable to promote an EMT (Fig. 4A, B) or induce ERM phosphorylation (Fig. 4C, D). PDPN-WT-mediated ERM phosphorylation was inhibited by treatment of the cells with CD (Fig. 4E, F), suggesting that for podoplanin to activate ERM its association with cholesterol-enriched DRMs is required.

PDPN-ECD, PDPN-CD45 and PDPN-TLR9 were also unable to stimulate MDCK cell migration, as shown in both Transwell and scratch assays (Fig. 5A, B). To further investigate the migratory behavior of MDCK cell transfectants, we tracked the migration pattern of a representative number of cells for each transfectant to study their random migration (Fig. 5C). PDPN-WT stimulated (~2 fold) the migration speed of MDCK cells (Fig. 5D): indeed control MDCK cells had an average speed of ~0.3 μm/min while that of cells expressing PDPN-WT was ~0.6 μm/min. Migration speeds for all MDCK cell chimeric transfectants were significantly reduced with respect to PDPN-WT expressing cells (Fig. 5D). In addition, we found that the movement of PDPN-WT- and PDPN-TLR9-MDCK cells were less random, more directional than that of cells expressing PDPN-ECD and PDPN-CD45 (Fig. 5E), and resulted in longer displacements for the former cell lines (Fig. 5F).

3.4. The GXXXG motif within the TM domain is essential for podoplanin homodimerization, association with DRM, and EMT

In experiments aimed at detecting the expression of podoplanin in human tissues by Western blotting, we noticed the presence of a form of ~80 kDa in addition to the reported mature form of ~ 38 kDa (see several examples in Fig. 6B). The 80-kDa band most probably to a podoplanin non-covalent homodimer, since it disappeared together with the 38-kDa band following preincubation of the anti-podoplanin antibody with the immunogenic peptide (Fig. 6B). Similar results have been found by Zimmer et al. (1999), both in MDCK type II cells expressing human podoplanin and MDCK type I cells expressing endogenous podoplanin. The TM domain of podoplanin is well conserved across species, particularly the region located at the N-terminus comprising a GXXXG motif (Fig. 6A and Table S2 in Supplementary material). GXXXG motifs have been involved in high affinity TM homomeric and heteromeric helix-helix associations (Russ and Engelman, 2000). Therefore, we analyzed podoplanin self-association by the TOXCAT assay that measures TM helix-helix association in the E. coli inner membrane (Russ and Engelman, 2000). As a positive control, we used a construct containing the M1 TM segment of ENAC (Kashlan et al., 2006). Bacteria harbouring PDPN-WT or ENAC were able to grow in chloramphenicol, in contrast to bacteria harbouring the empty vector (data not shown). These results were confirmed (Fig. 6C) in a second set of experiments by directly measuring luciferase activity with a modified version of pML27 in which CAT was replaced with luciferase (see Supplementary material). In these assays, we included a podoplanin construct with the TM GXXXG motif mutated to GXXXL (PDPN-G137L). In contrast to PDPN-WT, PDPN-G137L was unable to self-associate (Fig. 6C), indicating that the TM GXXXG motif is necessary for dimerization.

In order to ascertain whether this mutant protein was associated with DRM, we expressed PDPN-G137L as a fusion protein with eGFP in MDCK cells. As shown in Fig. 6D, PDPN-G137L did not float on an OptiPrep^{TM} density gradient, indicating that the G137L mutation blocks podoplanin association with the DRM fraction. Furthermore, this construct

was not recruited by CTB-coated beads (Fig. 3S). We next analyzed whether PDPN-G137L conserved the ability to promote an EMT. All analyzed clones transfected with PDPN-G137L exhibited an epithelial morphology. Expression of PDPN-G137L in these clones was rather heterogeneous, ranging from very low levels in some cells to high levels in others. However, even cells synthesizing high levels of PDPN-G137L had a polygonal morphology and preserved the expression of E-cadherin at cell-cell contacts. In addition, cells expressing PDPN-G137L had strong cortical F-actin bundles and short thin stress fibers, whereas cells expressing PDPN-WT exhibited weaker cortical F-actin and longer and thicker stress fibers typical of fibroblasts (Fig. 7A). Furthermore, the G137L mutation hampered podoplanin-mediated ERM phosphorylation, as shown by confocal immunofluorescence microscopy (Fig. 7B). These results suggest that mutation of the TM GXXXG motif impairs podoplanin self association, prevents its localization at cholesterol-rich membrane micro domains, and blocks podoplanin-mediated EMT.

4. Discussion

Lipid rafts platforms are specialized plasma membrane micro domains rich in cholesterol, sphingolipids and proteins (Simons and Toomre, 2000). Recent findings indicate that these structures are dynamic and heterogeneous, although some proteins are clearly "raftophylic" (Brown, 2006), like Cav-1 or prominin-1, (Roper et al., 2000). In this work, we show that human podoplanin expressed in MDCK cells associates with these structures, in accordance with its microvillar plasma membrane location (Scholl et al., 1999; Martin-Villar et al., 2005).

We have investigated the structural basis for podoplanin raft association by examining the detergent insolubility of several mutant constructs affecting its EC, TM and CT domains.

All mutant proteins, except for PDPN-ΔEC, lost the detergent-resistant properties exhibited by wild type podoplanin, indicating that both the TM and CT domains are required for podoplanin localization in lipid rafts. We had previously proposed a model in which the interaction of podoplanin with ezrin/moesin induced the activation of RhoA/ROCK, thus leading to further activation of ERM proteins and the induction of an EMT (Martín-Villar et al., 2006). We show in this work that disruption of lipid rafts by CD impairs podoplanin-mediated ERM phosphorylation. In addition, none of the podoplanin mutant proteins unable to include into rafts stimulated ERM phosphorylation, EMT or cell migration in MDCK cells. These results suggest that activation of ERM proteins and promotion of EMT by podoplanin requires its association with raft membrane micro domains. It has been shown that resistance to detergent extraction may vary depending on the cell type (Neame and Isacke, 1993); thus raising the possibility that the inability of podoplanin chimeras and the ΔCT mutant to associate with DRMs is due to the fact that these proteins retain the epithelial phenotype, whereas PDPN-WT and PDPN-ΔEC have a fibroblastic one. However, this argument can be ruled out as PDPN-ΔYS, a shorter podoplanin isoform (Martin-Villar et al., 2009) while unable to promote an EMT or activate ERM proteins in MDCK cells (M.M. Yurrita, J. Renart and M. Quintanilla, manuscript in preparation) is associated with the DRM fraction. This fact appears to indicate that DRM association is necessary but not sufficient for podopanin's effect on epithelial plasticity.

The requirement of the TM domain for podoplanin localization in cholesterol-rich membrane micro domains is probably due to direct protein-lipid interactions mediated by hydrophobic residues located mostly in the exoplasmic half of this domain as has been described for other proteins (Scheiffele et al., 1997). Several hypothesis can be proposed to explain the dependence of podoplanin raft localization on its CT domain. For instance, it has been shown that peptides with both basic and aromatic amino acid residues bind to

membranes (Arbuzova et al., 2000), and the podoplanin CT has this structure. On the other hand, we have previously described the anchorage of podoplanin to the actin cytoskeleton via its association with ezrin/moesin (Scholl et al., 1999; Martín-Villar et al., 2006), and ezrin is a predominantly raft protein (Gupta et al., 2006).Recent reports indicate that membrane rafts dynamics is controlled by proteins that are linked to the actin cytoskeleton (Viola and Gupta, 2007). Therefore, recruitment of podoplanin into lipid rafts could be necessary for its proper binding to ezrin and the actin cytoskeleton. Moreover, as has been described for CD44, and ERM-binding protein whose association with the actin cytoskeleton is regulated by lipid raft inclusion (Oliferenko et al., 1999), podoplanin inclusion into rafts could be important for the activation of the RhoA/ROCK pathway. In this regard, we have recently reported that podoplanin interacts with CD44 at plasma membrane protrusions (Martin-Villar et al., 2010).

The analysis of cell tracks during random migration revealed that PDPN-WT increased both the speed and directionality of MDCK cells. We also observe that PDPN-TLR9, which accumulated at intracellular vesicles, promoted a more directional movement while barely stimulating the speed of migration. The molecular bases for those observations are presently unknown. However, the fact that both PDPN-WT and PDPN-TLR9 were able to promote directionality during cell migration suggests that this function might involve podoplanin endocytosis or turnover from the cell surface. The subcellular distribution of PDPN-TLR9 corresponds to that of wild type TLR9 (Leifer et al., 2004). This result suggests that the TM domain of TLR9 is essential for its correct subcellular localization, which is in accordance with Kajita et al. (2006). However, other reports suggest that it is the CT domain and not the TM domain that controls the internal localization of TLR9 (Leifer et al., 2006). In this respect, it is worth mentioning that the opposite chimera, in which the TM domain of TLR9 was substituted by the TM region of podoplanin, is not directed to the cell surface but retained in the endoplasmic reticulum (data not shown), suggesting that neither the TM

domain of podoplanin nor that of TLR9 by themselves are sufficient for the subcellular distribution of the corresponding proteins.

The TM GXXXG motif appears to play an essential role in podoplanin's function and association with lipid rafts. The GXXXG motif has been established as a framework for the helix-helix interaction of TM domains and has been shown to mediate both homomeric and heteromeric association of TM helices (Gerber et al., 2004). Using a TOXLUC reporter system we indeed demonstrate that the TM GXXXG motif mediates podoplanin self-assembly in a membrane microenvironment. The GXXXG motif appears to be essential for podoplanin function since the PDPN-G137L mutant was unable to induce EMT or promote ERM phosphorylation. Altogether, these results suggest that TM mediated lateral clustering is important for retention of podoplanin in cholesterol-based membrane lipid rafts, which in turn may regulate podoplanin interaction with the actin cytoskeleton and podoplanin function. Currently, lipid rafts are viewed as dynamic nanoscale assemblies of sphingolipids, cholesterol and proteins that can coalesce by TM protein oligomerization into larger raft platforms stabilized by scaffolding elements, such as cortical actin (Lingwood and Simons, 2010). These platforms function in membrane signalling and may be required for specific events, such as EMT. Indeed, it has been recently reported that TGF-β-induced EMT is dependent on cholesterol-rich lipid rafts (Zuo and Chen, 2009). We provide in this work further evidence for the involvement of lipid rafts in EMT induction.

In summary, our results support that podoplanin is a raftophylic protein. Indeed, podoplanin is found in DRMs, and treatment with CD reduces its presence in these fractions. In addition, we have previously shown that podoplanin interacts with other raft proteins, like CD44 and ERMs, that also interact with the actin cytoskeleton. Both podoplanin and CD44 are able to signal via the RhoA/ROCK pathway. We observed a perfect correlation between the presence in DRMs and the ability to phosphorylate ezrin for all the podoplanin mutant and

chimeric proteins that we have studied. Furthermore this correlation is independent of the phenotype of the cells studied. Finally, we provide evidence for the involvement of the TM domain of podoplanin in its homodimerization via its GXXXG domain. This process, together with the interactions mentioned above, could enhance the formation of raft platforms and raft phases, likely involved in cell movement, in which podoplanin is clearly involved.

Acknowledgements

We thank Drs. Helen Yarwood, Amparo Cano, Francisco Sánchez-Madrid and Kenneth Blumenthal for their generous gifts of antibodies and plasmids. We also thank Dr. Miguel A. del Pozo (Centro Nacional de Investigaciones Cardiovasculares, Madrid, Spain) for his help with bead assays, and Dr. Eduardo Pérez-Gómez (Universidad Complutense, Madrid) for helpful suggestions. This work was supported by grants SAF2007-63821 and SAF2010-19152 from the Spanish Ministry of Science and Innovation. The support of Cancer Research UK to EM-V is also acknowledged. BF-M was the recipient of a predoctoral fellowship from the CSIC.

References

Arbuzova A, Wang L, Wang J, Hangyas-Mihalyne G, Murray D, Honig B, et al. Membrane binding of peptides containing both basic and aromatic residues. Experimental studies with peptides corresponding to the scaffolding region of caveolin and the effector region of MARCKS. Biochemistry 2000;39**,** 10330-9.

Atsumi N, Ishii G, Kojima M, Sanada M, Fujii S, Ochiai A. Podoplanin, a novel marker of tumor-initiating cells in human squamous cell carcinoma A431. Biochem Biophys Res Commun 2008;373**,** 36-41.

Barth K, Blasche R, Kasper M. T1alpha/podoplanin shows raft-associated distribution in mouse lung alveolar epithelial E10 cells. Cell Physiol Biochem 2010;25**,** 103-12.

Brown DA. Lipid rafts, detergent-resistant membranes, and raft targeting signals. Physiology (Bethesda) 2006;21**,** 430-9.

Crooks GE, Hon G, Chandonia JM, Brenner SE. WebLogo: a sequence logo generator. Genome Res 2004;14**,** 1188 - 90.

del Pozo MA, Alderson NB, Kiosses WB, Chiang HH, Anderson RG, Schwartz MA. Integrins regulate Rac targeting by internalization of membrane domains. Science 2004;303**,** 839-42.

Francis SA, Kelly JM, McCormack J, Rogers RA, Lai J, Schneeberger EE, et al. Rapid reduction of MDCK cell cholesterol by methyl-beta-cyclodextrin alters steady state transepithelial electrical resistance. Eur J Cell Biol 1999;78**,** 473-84.

Gerber D, Sal-Man N, Shai Y. Two motifs within a transmembrane domain, one for homodimerization and the other for heterodimerization. J Biol Chem 2004;279**,** 21177-82.

Gomez-Mouton C, Abad JL, Mira E, Lacalle RA, Gallardo E, Jimenez-Baranda S, et al. Segregation of leading-edge and uropod components into specific lipid rafts during T cell polarization. Proc Natl Acad Sci U S A 2001;98**,** 9642-7.

Gupta N, Wollscheid B, Watts JD, Scheer B, Aebersold R, DeFranco AL. Quantitative proteomic analysis of B cell lipid rafts reveals that ezrin regulates antigen receptor-mediated lipid raft dynamics. Nat Immunol 2006;7**,** 625-33.

Kajita E, Nishiya T, Miwa S. The transmembrane domain directs TLR9 to intracellular compartments that contain TLR3. Biochem Biophys Res Commun 2006;343**,** 578-84.

Kashlan OB, Maarouf AB, Kussius C, Denshaw RM, Blumenthal KM, Kleyman TR. Distinct structural elements in the first membrane-spanning segment of the epithelial sodium channel. J Biol Chem 2006;281**,** 30455-62.

Kunita A, Kashima TG, Morishita Y, Fukayama M, Kato Y, Tsuruo T, et al. The platelet aggregation-inducing factor aggrus/podoplanin promotes pulmonary metastasis. Am J Pathol 2007;170**,** 1337-47.

Leifer CA, Kennedy MN, Mazzoni A, Lee C, Kruhlak MJ, Segal DM. TLR9 is localized in the endoplasmic reticulum prior to stimulation. J Immunol 2004;173**,** 1179-83.

Leifer CA, Brooks JC, Hoelzer K, Lopez J, Kennedy MN, Mazzoni A, et al. Cytoplasmic targeting motifs control localization of toll-like receptor 9. J Biol Chem 2006;281**,** 35585-92.

Lingwood D, Simons K. Lipid rafts as a membrane-organizing principle. Science 2010;327**,** 46-50.

Lis M, Blumenthal K. A modified, dual reporter TOXCAT system for monitoring homodimerization of transmembrane segments of proteins. Biochem Biophys Res Commun 2006;339**,** 321-4.

Mahtab EA, Wijffels MC, Van Den Akker NM, Hahurij ND, Lie-Venema H, Wisse LJ, et al. Cardiac malformations and myocardial abnormalities in podoplanin knockout mouse embryos: Correlation with abnormal epicardial development. Dev Dyn 2008;237**,** 847-57.

Martin-Villar E, Scholl FG, Gamallo C, Yurrita MM, Munoz-Guerra M, Cruces J, et al. Characterization of human PA2.26 antigen (T1alpha-2, podoplanin), a small membrane mucin induced in oral squamous cell carcinomas. Int J Cancer 2005;113**,** 899-910.

Martin-Villar E, Yurrita MM, Fernandez-Munoz B, Quintanilla M, Renart J. Regulation of podoplanin/PA2.26 antigen expression in tumour cells. Involvement of calpain-mediated proteolysis. Int J Biochem Cell Biol 2009;41**,** 1421-9.

Martin-Villar E, Fernandez-Munoz B, Parsons M, Yurrita MM, Megias D, Perez-Gomez E, et al. Podoplanin Associates with CD44 to Promote Directional Cell Migration. Mol Biol Cell 2010;

Martín-Villar E, Megias D, Castel S, Yurrita MM, Vilaro S, Quintanilla M. Podoplanin binds ERM proteins to activate RhoA and promote epithelial-mesenchymal transition. J Cell Sci 2006;119**,** 4541-53.

Neame SJ, Isacke CM. Phosphorylation of CD44 in vivo requires both Ser323 and Ser325, but does not regulate membrane localization or cytoskeletal interaction in epithelial cells. EMBO J 1992;11**,** 4733-8.

Neame SJ, Isacke CM. The cytoplasmic tail of CD44 is required for basolateral localization in epithelial MDCK cells but does not mediate association with the detergent-insoluble cytoskeleton of fibroblasts. J Cell Biol 1993;121**,** 1299-310.

Oliferenko S, Paiha K, Harder T, Gerke V, Schwarzler C, Schwarz H, et al. Analysis of CD44-containing lipid rafts: Recruitment of annexin II and stabilization by the actin cytoskeleton. J Cell Biol 1999;146**,** 843-54.

Ordonez NG. Podoplanin: a novel diagnostic immunohistochemical marker. Adv Anat Pathol 2006;13**,** 83-8.

Patra SK. Dissecting lipid raft facilitated cell signaling pathways in cancer. Biochim Biophys Acta 2008;1785**,** 182-206.

Poole K, Meder D, Simons K, Muller D. The effect of raft lipid depletion on microvilli formation in MDCK cells, visualized by atomic force microscopy. FEBS Lett 2004;565**,** 53-8.

Ramirez MI, Millien G, Hinds A, Cao Y, Seldin DC, Williams MC. T1alpha, a lung type I cell differentiation gene, is required for normal lung cell proliferation and alveolus formation at birth. Dev Biol 2003;256**,** 61-72.

Roper K, Corbeil D, Huttner WB. Retention of prominin in microvilli reveals distinct cholesterol-based lipid micro-domains in the apical plasma membrane. Nat Cell Biol 2000;2**,** 582-92.

Russ WP, Engelman DM. The GxxxG motif: a framework for transmembrane helix-helix association. J Mol Biol 2000;296**,** 911-9.

Schacht V, Ramirez MI, Hong YK, Hirakawa S, Feng D, Harvey N, et al. T1α/podoplanin deficiency disrupts normal lymphatic vasculature formation and causes lymphedema. EMBO J 2003;22**,** 3546-56.

Scheiffele P, Roth MG, Simons K. Interaction of influenza virus haemagglutinin with sphingolipid-cholesterol membrane domains via its transmembrane domain. EMBO J 1997;16**,** 5501-8.

Scholl FG, Gamallo C, Vilaró S, Quintanilla M. Identification of PA2.26 antigen as a novel cell-surface mucin-type glycoprotein that induces plasma membrane extensions and increased motility in keratinocytes. J Cell Sci 1999;112 (Pt 24)**,** 4601-13.

Scholl FG, Gamallo C, Quintanilla M. Ectopic expression of PA2.26 antigen in epidermal keratinocytes leads to destabilization of adherens junctions and malignant progression. Lab Invest 2000;80**,** 1749-59.

Simons K, Toomre D. Lipid rafts and signal transduction. Nat Rev Mol Cell Biol 2000;1**,** 31-9.

Simons K, Gerl MJ. Revitalizing membrane rafts: new tools and insights. Nat Rev Mol Cell Biol 2010;11**,** 688-99.

Viola A, Gupta N. Tether and trap: regulation of membrane-raft dynamics by actin-binding proteins. Nat Rev Immunol 2007;7**,** 889-96.

Wicki A, Lehembre F, Wick N, Hantusch B, Kerjaschki D, Christofori G. Tumor invasion in the absence of epithelial-mesenchymal transition: podoplanin-mediated remodeling of the actin cytoskeleton. Cancer Cell 2006;9**,** 261-72.

Wicki A, Christofori G. The potential role of podoplanin in tumour invasion. Br J Cancer 2007;96**,** 1-5.

Zimmer G, Lottspeich F, Maisner A, Klenk HD, Herrler G. Molecular characterization of gp40, a mucin-type glycoprotein from the apical plasma membrane of Madin-Darby canine kidney cells (type I). Biochem J 1997;326 (Pt 1)**,** 99-108.

Zimmer G, Oeffner F, Von Messling V, Tschernig T, Groness HJ, Klenk HD, et al. Cloning and characterization of gp36, a human mucin-type glycoprotein preferentially expressed in vascular endothelium. Biochem J 1999;341 (Pt 2)**,** 277-84.

Zuo W, Chen YG. Specific activation of mitogen-activated protein kinase by transforming growth factor-beta receptors in lipid rafts is required for epithelial cell plasticity. Mol Biol Cell 2009;20**,** 1020-9.

Figure captions

Fig. 1. Podoplanin is associated with the detergent-resistant cholesterol-rich membrane fraction. (A) MDCK cells expressing wild type PDPN fused to eGFP were lysed at 4ºC in 0.2% Triton X-100 and the levels of podoplanin in the soluble (S) and insoluble (I) fractions were determined by Western blotting. α-tubulin and cytokeratin 8 (CK8) were used as controls for soluble and insoluble proteins, respectively. (B) MDCK cells expressing wild-type PDPN fused to eGFP were treated with CD or vehicle and lysed at 4ºC in 0.5% Triton X-

100. Cell lysates were subjected to flotation on OptiPrep^{TM} density gradients, and the expression levels of PDPN, CD44 and caveolin-1 (Cav-1) in the gradient fractions determined by Western blotting. Fractions 1-8 represent low (0%) to high (35% Optiprep) density. TL, total lysate. (C) Recruitment of both PDPN and CD44 by CTB-coated beads. MDCK-PDPN-eGFP cells plated on coverslips were incubated with 5-μm polystyrene beads coated with CTB or α-TrfR (negative control) for 15 min. Cells were then processed for immunofluorescence to detect CD44.

Fig. 2. Subcellular localization of PDPN wild-type and mutant proteins. Confocal images of horizontal sections of MDCK cells expressing the indicated PDPN constructs fused to eGFP are shown. Protein specifically expressed at the cell surface was detected by in vivo preembedding staining using an antibody recognizing the EC domain of PDPN. Inset in PDPN-TLR9 indicates localization of the mutant protein at internal vesicles (arrow). Bars, 25 μm.

Fig. 3. Detergent insolubility properties of podoplanin mutant proteins. MDCK cells expressing wild-type and the indicated mutant PDPN proteins fused to eGFP were lysed at 4ºC in either 0.2% (A) or 0.5% (B) Triton X-100 and processed as indicated in the legend of Fig. 1. In panel A, the ratio of insoluble to soluble fraction loaded onto the gel was 4:1 in order to better visualize changes in Triton X-100 insolubility of mutant proteins with respect to wild type PDPN. In panel B, fractions 1-8 represent low (0%) to high (35% Optiprep) density.

Fig. 4. The TM domain is important for podoplanin-induced EMT. (A) Phase contrast micrographs of MDCK cells expressing the indicated constructs. (B) Western blot analysis of

PDPN proteins and of the differentiation-related markers E-cadherin (E-CD) and N-cadherin (N-CD) in MDCK cells transfected with the indicated constructs or the empty vector (eGFP). Two different clones per each PDPN chimeric mutant are shown. α-tubulin was a used as a control for protein loading. (C) Representative western blot analysis of phospho-ERM and total ezrin levels in the indicated MDCK cell transfectants. (D) Quantification of ERM protein activation, expressed as P-ERM over total ezrin levels, in TM chimeras (n=6). (E) Representative western blot analysis of phospho-ERM and total ezrin levels in MDCK cells transfected with the empty vector (eGFP) and wild type PDPN before and after treatment with CD. (F) Quantification of ERM protein activation relative to control cells after treatment with CD, expressed as ERM activation over ERM activation in MDCK-eGFP cells (n=3). P-values (panels D and F) were obtained using a one-way analysis of variance (ANOVA) with a Bonferroni post-test and the Student's *t*-test respectively: *p<0.05; **p<0.01; ***p<0.001.

Fig. 5. Substitution of the TM domain of podoplanin impairs cell migration. (A) Transwell migration assay of MDCK cells transfected with the indicated constructs. (B) Wound healing assay. MDCK cells expressing PDPN-WT closed completely a wound made 12 h before while control cells (eGFP) and cells expressing PDPN mutant proteins did not. (C-F) Random cell migration assay. The traces of the movement of a representative number of cells (n = 20) during a 15 h period for the indicated transfectants are represented as wind-rose plots (C). For mean migration speed (D), directionality (E) and displacement (F) determinations, the number of cells tracked was as follow: eGFP), n = 65; PDPN-WT, n = 42; PDPN-ECD, n = 63; PDPN-CD45, n = 25; PDPN-TLR, n = 92. Bar graphs (mean $\pm$ s.e.m.) are representative of three independent experiments. P-values were obtained using the Student's *t*-test. **p<0.01; ***p<0.001.

Fig. 6. A GXXXG motif within the TM region is involved in podoplanin homodimerization and association with the DRM fraction. (A) Sequence Logo (Crooks et al., 2004) generated from the alignment of the TM domain of podoplanin from the different species shown in Table S2. The human TM sequence of podoplanin (with the GXXXG motif underlined) is presented below. (B) Western blot analysis of podoplanin expressed in human normal and tumor tissues using an antibody preincubated or not with the immunogenic peptide (P37-51) to detect podoplanin specific forms. CRC, colorectal carcinoma. (C) TOXLUC assay to measure homodimerization of the indicated TM domains at the inner membrane of E. coli. ENAC was used as a positive control. Note that mutation of the last G in the GXXXG motif (G137L) inhibits podoplanin homodimerization. Results are the mean of three independent biological experiments carried out in triplicate. P-values were obtained using a one-way analysis of variance (ANOVA) with a Bonferroni post-test. *$p<0.05$; **$p<0.01$. (D) The G137L mutation blocks PDPN association with the DRM fraction. The lysates of MDCK cells expressing either the PDPN-WT or PDPN-G137L mutant proteins obtained as described in the legend of Figure 1B were subjected to flotation on OptiPrep^{TM} density gradient, and the expression of PDPN and Cav-1 determined in the gradient fractions by Western blotting.

Fig. 7. Mutation of the TM GXXXG motif prevents podoplanin-mediated ERM phosphorylation and EMT. Confocal fluorescence detection of E-cadherin and F-actin (A) and of phospho-ERM proteins (B) in MDCK cells expressing PDPN-WT and mutant PDPN-G137L fused to eGFP. Cells were labelled with specific antibodies against E-cadherin (E-CD) and phosphor-ERM or with Alexa Fluor coupled to phalloidin. Nuclei were stained with DAPI. In panel B, laser intensity and gain were adjusted for PDPN-WT and maintained for PDPN-G137L.

Figure(s)

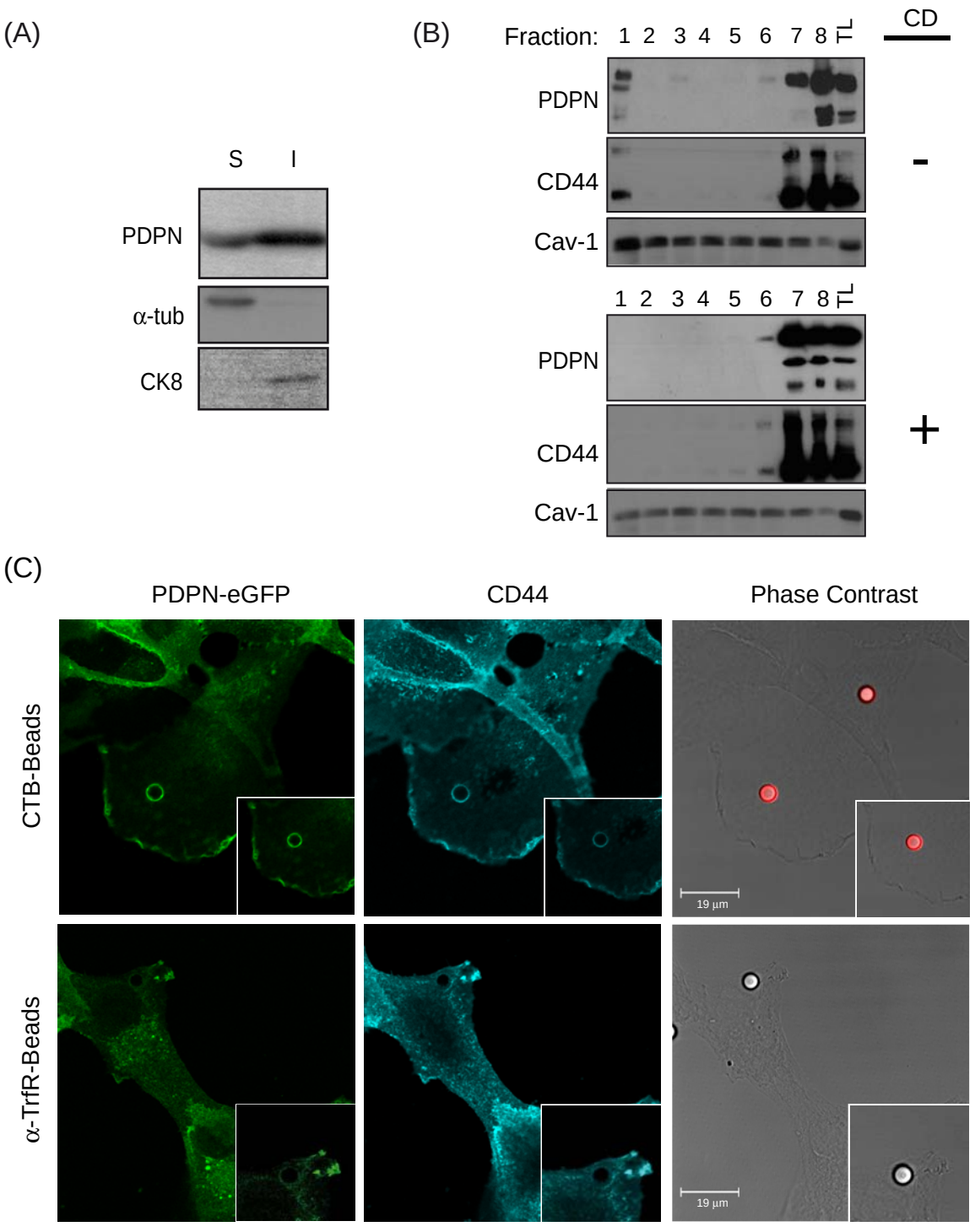

Fernandez-Muñoz et al, Figure 1

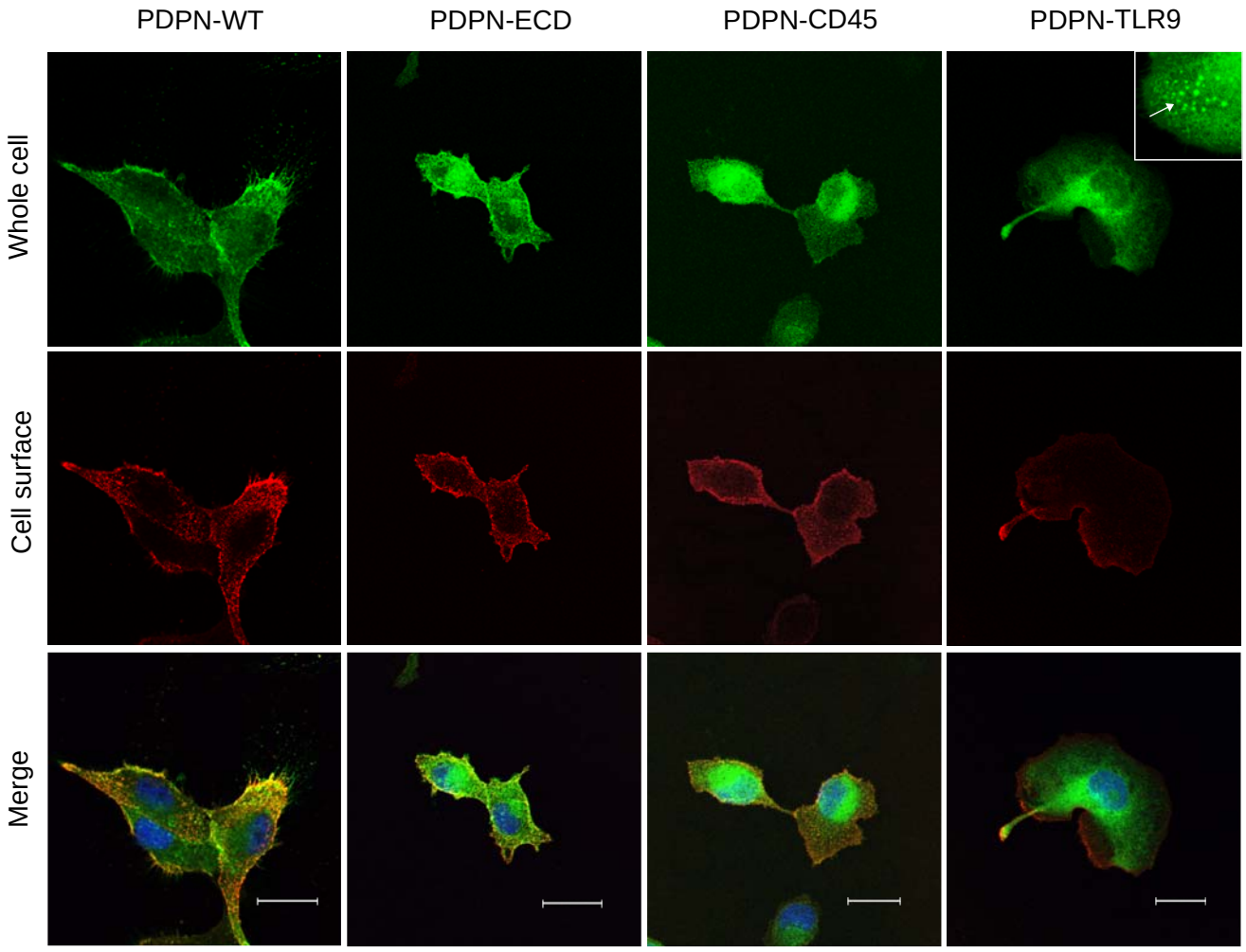

Fernandez-Muñoz et al, Figure 2

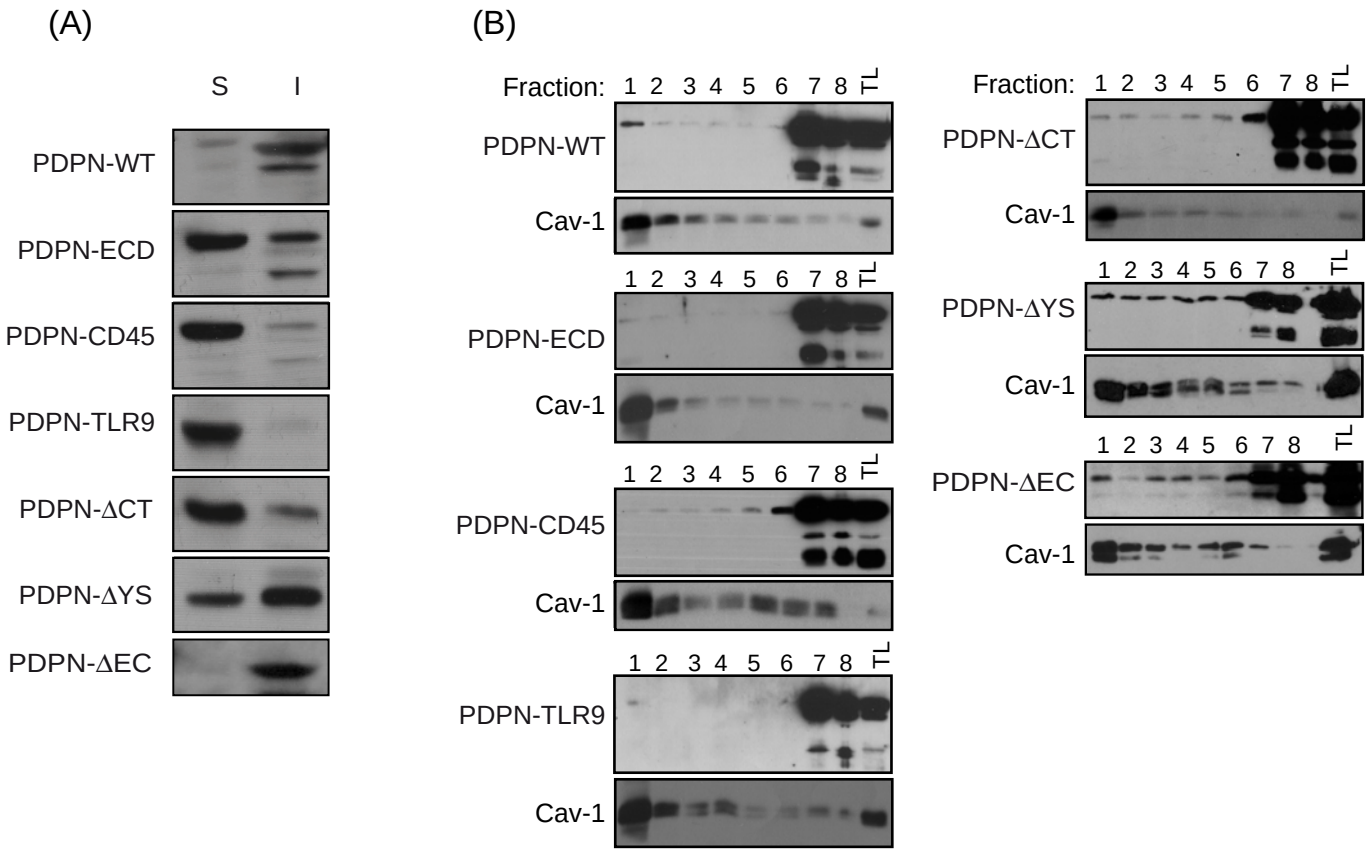

Fernandez-Muñoz et al, Figure 3

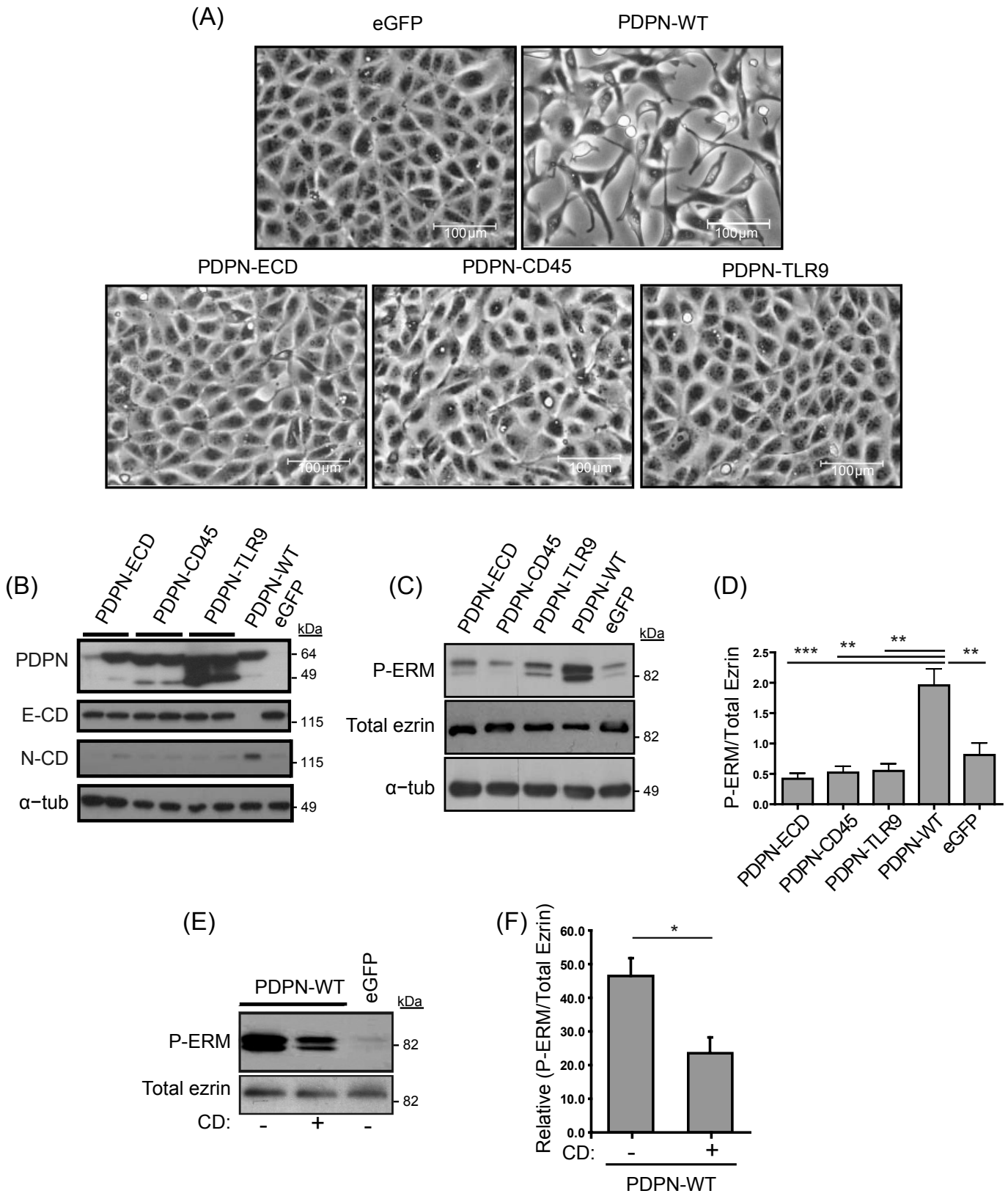

Fernandez-Muñoz et al, Figure 4

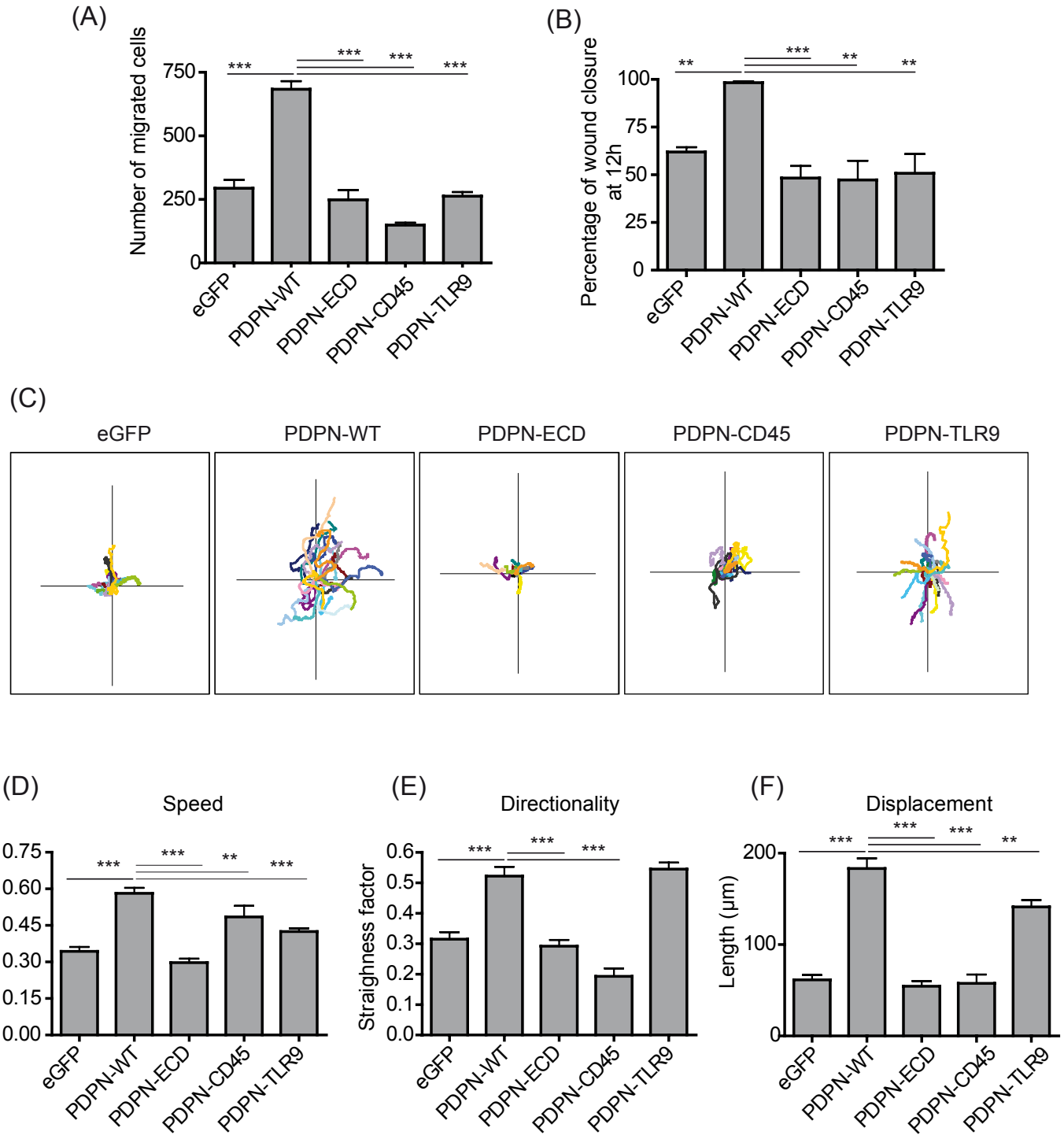

Fernandez-Muñoz et al, Figure 5

(A)

Human PDPN: VTLVGIIVGVLLAIGFIGAIIVVVM

(B)

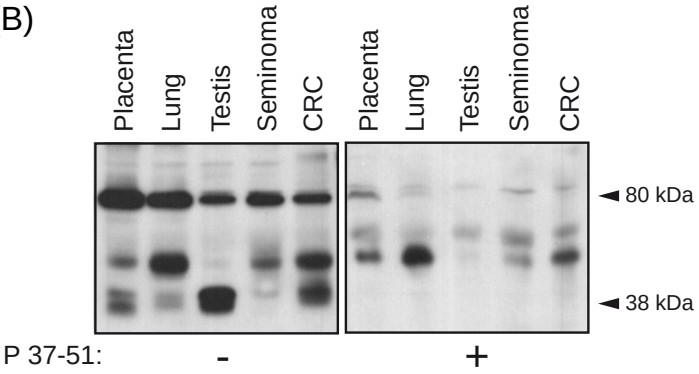

(C)

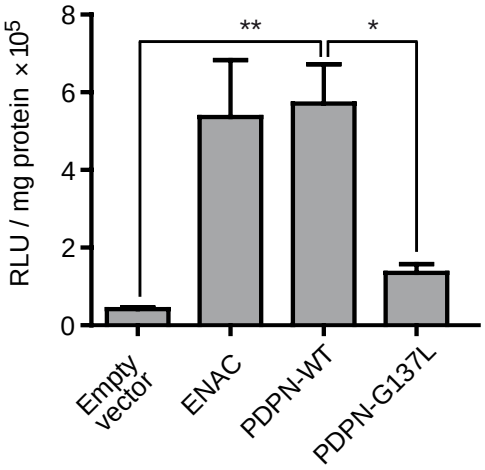

(D)

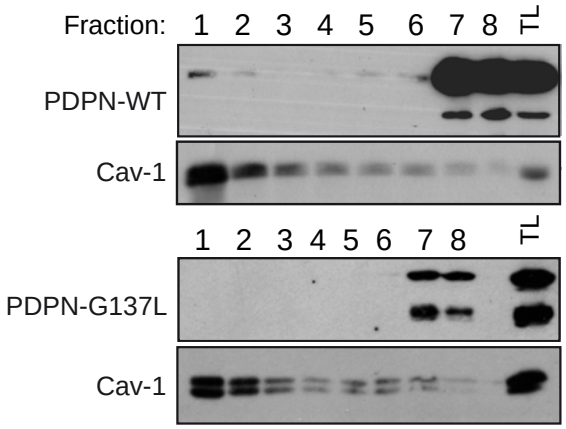

Fernandez-Muñoz et al, Figure 6

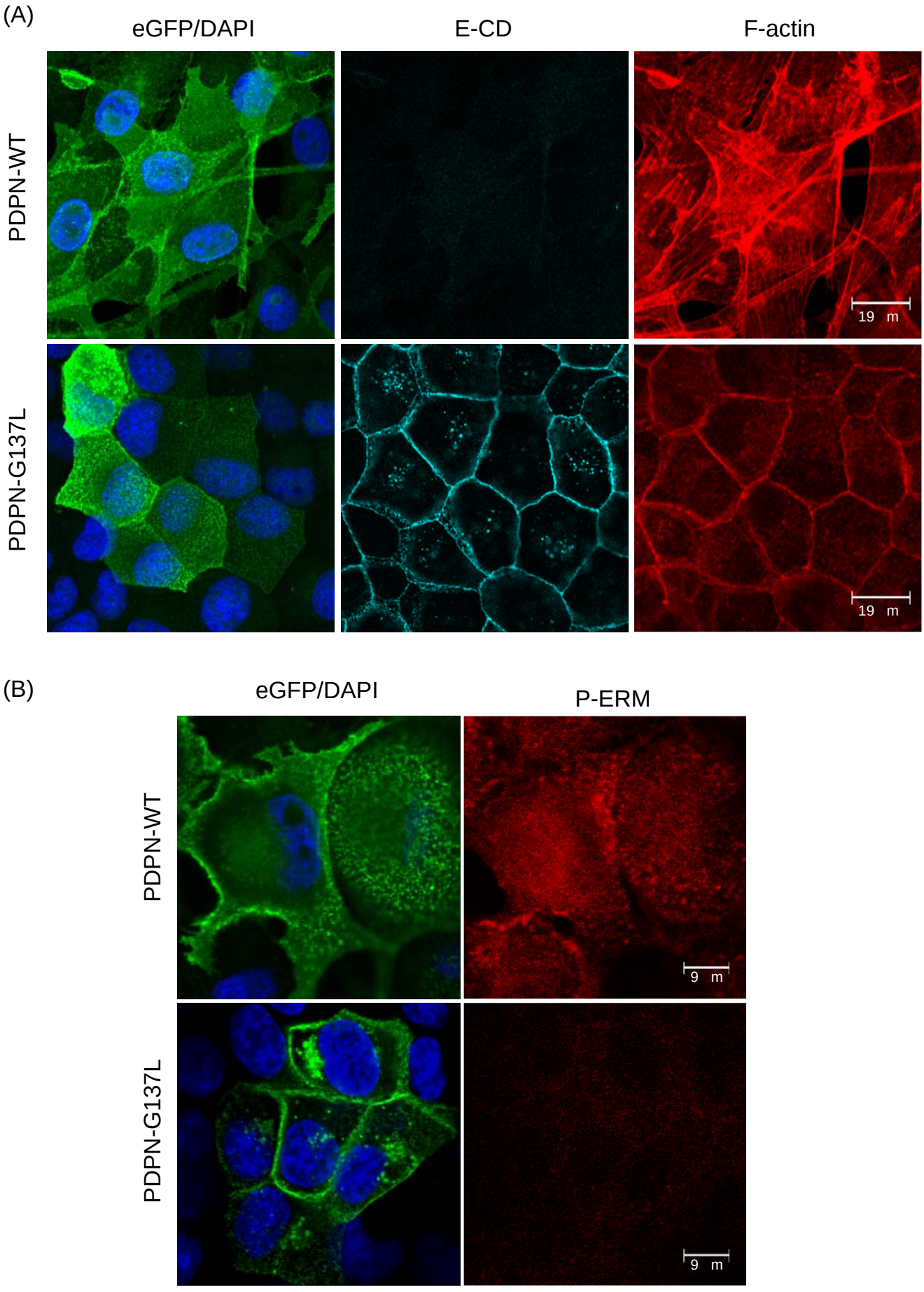

Fernandez-Muñoz et al, Figure 7

Supplementary Files

Click here to download Supplementary Files: Fernandez-Muoz_et_al_Suppl_Material.pdf